THE JOURNAL OF PHYSICAL CHEMISTRY B

ARTICLE

pubs.acs.org/JPCB

Conformational Study of the Hydroxyproline−O−Glycosidic Linkage: Sugar−Peptide Orientation and Prolyl Amide Isomerization in (α/β)−Galactosylated 4(*R*/*S*)−Hydroxyproline

Emmanuel B. Naziga,[†] Frank Schweizer,[‡] and Stacey D. Wetmore*[,†]

[†]Department of Chemistry and Biochemistry, University of Lethbridge, 4401 University Drive, Lethbridge, Alberta, Canada T1K 3M4

[‡]Department of Chemistry, University of Manitoba, Winnipeg, Manitoba, Canada R3T 2N2

Supporting Information

ABSTRACT: Glycosylation is a frequent post-translational modification of proteins that has been shown to influence protein structure and function. Glycosylation of hydroxyproline occurs widely in plants, but is absent in humans and animals. Previous experimental studies on model amides have indicated that α/β-galactosylation of 4*R*-hydroxyproline (Hyp) has no measurable effect on prolyl amide isomerization, while a 7% increase in the *trans* isomer population, as well as a 25−50% increase in the isomerization rate, was observed for the 4S stereoisomer (hyp). In this work, molecular dynamics simulations in explicit water and implicit solvent DFT optimizations are used to examine the structure of the hydroxyproline−*O*−galactosyl linkage and the effect of glycosylation on the structure and *cis*/*trans* isomerization of the peptide backbone. The calculations show two major minima with respect to the glycosidic linkage in all compounds. The C^{γ}-exo puckering observed in 4R compounds projects the sugar away from the peptide backbone, while a twisted C^{γ}-endo/C^{β}-exo pucker in the 4S compounds brings the peptide and sugar rings together and leads to an intramolecular hydrogen-bonding interaction that is sometimes bridged by a water molecule. This hydrogen bond changes the conformation of the peptide backbone, inducing a favorable $n \rightarrow \pi^*$ interaction between the oxygen lone pair from the prolyl N-terminal amide and the C═O, which explains the observed increase in *trans* isomer population in α/β-galactosylated 4*S*-hydroxyproline. Our results provide the first molecular level information about this important glycosidic linkage, as well as provide an explanation for the previously observed increase in *trans* isomer population in 4S-hyp compounds. Moreover, this study provides evidence that sugar-mediated long-range hydrogen bonding between hydroxyl groups and the carbonyl peptide backbone can modify the properties of N-terminal prolyl *cis*/*trans* isomerization in peptides.

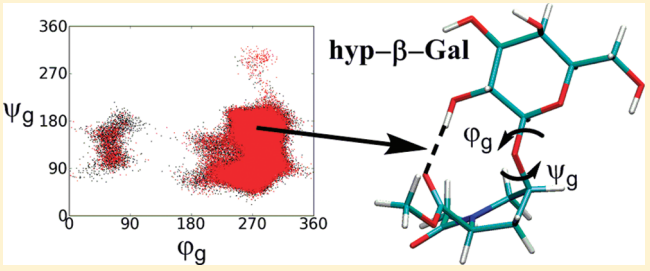

INTRODUCTION

Glycosylation is a common post-translational modification of proteins.[1−3] Aside from being involved in protein−carbohydrate recognition,[4−7] glycosylation also affects protein conformation and folding[4,5] and receptor binding and signaling,[4,5] facilitates membrane penetration,[8,9] enhances thermal stability[10,11] and resistance to proteolytic degradation,[12] and affects the hydration state of peptides.[13] Over the years, many small-model glycopeptides have been prepared to study how glycosylation affects peptide backbone conformation.[14,15] These studies have concluded that the nature of the glycosidic linkage not only influences the relative orientation of the sugar and peptide but also influences peptide backbone conformation and hence peptide properties.[16−19]

In animals and humans, carbohydrates are typically O-linked to serine (Ser) and threonine (Thr) or N-linked to asparagine (Asn).[5,20] In the plant kingdom, O-glycosylation of (2*S*,4*R*)-4-hydroxyproline or Hyp (Scheme 1) is widespread.[21] For example, O-glycosylation occurs in hydroxyproline-rich glycoproteins (HRGPs) that are associated with the cell walls of algae and flowering plants.[22−30] The Hyp−O−linked glycans are generally characterized by β-glycosidic linkages to either L-arabinose or D-galactose. Depending on the HRGP subclass, the glycan moiety may be a mono-, oligo-, or polysaccharide. However, the function of the attached glycan is still not completely understood. It has been recently found that the contiguous O-glycosylation of (2*S*,4*R*)-4-hydroxyproline in a nonaproline peptide dramatically enhances the thermal stability.[31] Molecular modeling suggests that the stabilization is the result of multiple interglycan and glycan−peptide backbone hydrogen bonds.[31] In contrast, the stereoisomer of Hyp, (2*S*,4*S*)-4-hydroxyproline (hyp, Scheme 1), is rarely found in nature, but has been isolated from extracts of the sandalwood tree *Santalum album*, several species of fungi, and the cyanobacteria *Lyngbya majuscula*.[32]

Received: August 4, 2011
Revised: November 29, 2011
Published: December 08, 2011

Glycosylation of Hyp and hyp is of particular interest since both proline analogues exhibit properties unique among proteinogenic amino acids. Specifically, proline and hydroxyproline have limited rotation about the ϕ ($\angle$(C1−C$^{\alpha}$−N−C), Schemes 2 and 3) dihedral angle because their side chains are fused to the peptide backbone. As a result, there is a reduction in the energy difference between the prolyl amide *cis* (ω = 0°) and *trans* (ω = 180°) isomers, which makes them nearly isoenergetic,[33−35] and leads to a higher *cis* N-terminal amide isomer content compared with other amino acids. Due to this structural feature, proline (Pro) and derivatives perform some distinct functions in proteins and peptides. For instance, prolyl *cis*/*trans* isomerization is often the rate-determining step in the folding pathways of many peptides (proteins),[33,36] and induces β-turns and extended helical structures (polyproline helices). It is also crucial in protein−protein interactions,[37−42] and plays an important role in the stabilities of structural proteins such as collagens[43,44] and extensins.[45−47]

Several factors govern the *cis*/*trans* isomerization equilibrium of Pro-based peptides[48,49] including an n → π^* interaction between the oxygen lone pair from the prolyl N-terminal amide C═O and the antibonding orbital of the C-terminal C═O (Scheme 2),[33−35,48−52] as well as inductive and stereoelectronic effects.[53−58] 4-Hydroxylation and attachment of other electron-withdrawing groups have a further influence on *cis*−*trans* isomerization by affecting the n → π^* interaction through changes in the conformation of the pyrrolidine ring (puckering) and the prolyl backbone ψ dihedral angle.[59] Glycosylation can also affect *cis*/*trans* isomerization in peptides. For instance, Ser O-glycosylation with either α-linked *N*-acetylgalactosamine or β-linked *N*-acetylglucosamine N-terminal to Pro stabilizes the *trans* amide conformation.[18] Previous experimental work has shown that glycosylation has no measurable influence on amide isomerization in Hyp,[60] but glycosylation affects both the N-terminal amide equilibrium and the rate of amide isomerization of hyp.[61] Indeed, both α- and β-anomeric galactosyl linkages to hyp stabilize the *trans* amide conformation by 7% relative to the ungalactosylated case in model amides. The reason for this experimental observation is not clear, but could involve differences in the orientation of the sugar with respect to the peptide in Hyp and hyp. Therefore, detailed molecular level information about the conformation and other implications of this glycosidic linkage is required to explain experimental findings.

As a result, several computational studies of the structural properties of hydroxyproline-based models have appeared in the literature.[62−69] For example, calculations on 4-hydroxyproline and 4-flouroproline provided evidence for previous experimental observations[54] that 4R electronegative substituents induce *exo* puckering, while 4S substituents induce *endo* puckering.[62] Additionally, 4R-electronegative elements stabilize the *trans* conformation, with stability increasing with electronegativity,[62] while 4S-substituents destabilize the *trans* conformation unless a hydrogen bond forms between the 4S-substituent and the C-terminal carbonyl, such as for 4*S*-hydroxyproline. Song and Kang examined the transition between *exo* and *endo* ring conformations in Hyp via an intermediate with an envelope pucker.[63] By studying the structure and amide isomerization of *N*-acetyl-4-hydroxyproline models, Aliev et al. noted that a tetrahedral geometry of the nitrogen atom at the transition state is an important structural feature of this *cis*/*trans* transformation.[64,65] Calculations revealed that a hydrogen bond between the 4S hydroxyl group and the peptide backbone could explain an increase in the *trans* to *cis* isomer ratio in $CDCl_3$.[66] Similarly, studies on a [(4*S*)NHAc-Pro]−OCH_3 model with a 4S *N*-acetyl group found very high *trans* isomer stability due to strong interactions with the acetamide at C4 and the C-terminal carbonyl group of the methyl ester.[67] Finally, Teklebrhan et al. determined that at least implicit solvation effects are necessary for correctly calculating the *cis*−*trans* distribution in glucosyl 3*S*-hydroxy-5-hydroxymethylproline hybrids.[68,69] In terms of elucidating the structural details of protein−sugar glycosidic linkages, Avenoza and co-workers have computationally examined O-glycosylation of model glycopeptides to explain differences in

Scheme 1. Compounds Considered in the Present Study

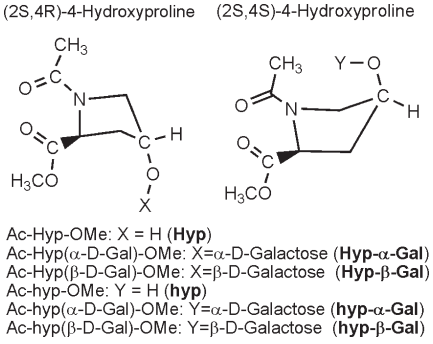

Scheme 2. Proline *Cis* Amide Isomer Depicting Relevant Backbone Torsional Angles and the *Trans* Amide Isomer with the n → π^* Interaction (Red Arrow) between the N-terminal Amide Carbonyl Oxygen and the C-terminal Carbonyl Carbon

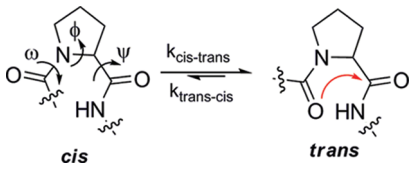

Scheme 3. Chemical Numbering and Definitions of Various Dihedral Angles in the Glycopeptides

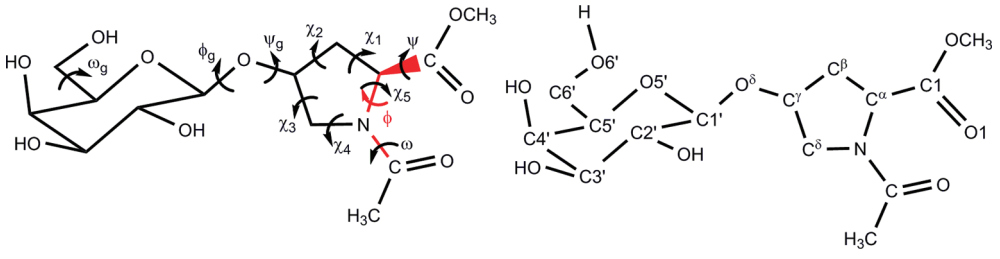

dx.doi.org/10.1021/jp207479q |*J. Phys. Chem. B* 2012, 116, 860–871

the conformation of an α-linked sugar to Ser and Thr.[70−72] Similarly, Ali et al. studied asparagine N-glycosylation with N-acetylated glucose and revealed that the *N*-acetyl group is important for the rigidity of the glycosidic linkage.[73] However, there is no study in the literature of the hydroxyproline O-glycosidic linkage, which is of importance to the structure of plant HRGPs.

The present work applies a combined quantum and molecular mechanical approach to examine the conformational properties of the two hydroxyproline stereoisomers: (i) *N*-acetyl-(2*S*,4*R*)-4-hydroxyproline methyl ester (Hyp) and (ii) *N*-acetyl-(2*S*,4*S*)-4-hydroxyproline methyl ester (hyp) together with their α/β-galactosylated derivatives (Scheme 1). In particular, we focus on the conformation of the Hyp (hyp)−O−glycosidic linkage, the effects of glycosylation on the structure and hydration of the peptide backbone, and deviations in the *cis*/*trans* isomerization upon glycosylation. Although (hydroxy) proline is fairly rigid, a dynamical methodology must be used since the glycopeptide includes a carbohydrate moiety with inherent flexibility. Additionally, the solvent environment must be carefully modeled since the presence of solvent (water) has been previously shown to be required to correctly sample the rotamers of exocyclic hydroxyls,[74] and the *cis*/*trans* distribution in related compounds.[69] Therefore, a two-pronged approach is implemented, which includes molecular dynamics (MD) simulations with explicitly included solvent molecules and density functional theory (DFT) based quantum mechanical calculations with implicit solvation effects. Our calculations reveal details of the Hyp (hyp)−galactose glycosidic linkage that are important for understanding the structure of HRGPs, clarify the implications of glycosylation on the peptide backbone, and provide a possible explanation for the experimentally reported changes in the thermodynamics and kinetics of *cis*/*trans* isomerization of hyp (but not Hyp) upon glycosylation.

COMPUTATIONAL DETAILS

Molecular Dynamics Simulations. Initial structures of all compounds under investigation (Scheme 1) were created with the XLeap module of the AMBER software suite.[75,76] The ff99SB AMBER force field parameter set[77] was used for the peptide, including an additional dihedral parameter developed by Park et al.[78] to account for the gauche effect in Hyp. The GLYCAM06 (version 06c) parameter set[79] was used for the galactose sugar, including the glycosidic-linkage dihedral parameters. Additional RESP derived charges for the methoxy (OMe) fragment were obtained using standard AMBER protocols.[80,81] To establish the glycosidic linkage between the sugar and peptide, the partial charge on the hydroxyl hydrogen was added to the linking oxygen and subsequently adjusted to yield a net neutral charge in accordance with standard GLYCAM procedure.[79] This approach led to a partial charge of −0.4223 which is similar to that previously used to describe other ester oxygens.[79]

Starting structures were solvated in a periodic octahedron of TIP3P water molecules. Once built, the models were subjected to two rounds of geometry optimizations. In the first round, the solute was held fixed by positional restraints while the solvent molecules were allowed to relax in 1000 minimization steps, which consist of 500 steepest descent (SD) steps before switching to the conjugate gradient (CG) method. In the second round, the structure output from the first round was further minimized with the same number of SD and CG steps without restraining the solute. Next, the system was heated for 20 ps from a randomly assigned initial temperature of 5 K to the desired temperature of 300 K. During this calculation, the solute was fixed with weak positional restraints. The final result from this simulation was used as a starting point for subsequent calculations in the constant pressure (NPT) ensemble. For all model compounds, a minimum 200 ns MD simulation at 300 K and 1 atm was carried out with the first 5 ns discarded as equilibration. A time step of 1.0 fs was used in the heating equilibration, while constant pressure equilibration/production calculations utilized a 2.0 fs time step. Temperature was controlled using a Langevin thermostat with a 1.0 ps time constant. Long-range electrostatic interactions were treated with the particle mesh Ewald (PME) summation, while a cutoff of 8 Å was used for nonbonded interactions. Scale factors of 2.0 and 1.2 were applied to the electrostatic and 1−4 van der Waals interactions, respectively, for the AMBER force field.[80] Although GLYCAM parameters are often also scaled using these same AMBER scale factors,[82] this approach is known to lead to improper sampling of some glycosidic dihedral angles[74,79] and therefore the GLYCAM parameters were not scaled. The SHAKE algorithm[83] was implemented to restrain all bonds involving hydrogen. MD calculations were performed with the PMEMD module of AMBER (version 10).[84]

Density Functional Theory Calculations. Minimum structures obtained from MD simulations were further optimized with B3LYP/6-311++G(d,p), and frequency calculations at the same level of theory were conducted to ensure that minima were obtained. B3LYP was used since this functional has been extensively applied in the literature to study proline peptides and carbohydrates.[63,85−90] The ϕ_g ($\angle$(O5′−C1′−O$^{\delta}$−C$^{\gamma}$)) and ψ_g ($\angle$(C$^{\beta}$−C$^{\gamma}$−O$^{\delta}$−C1′)) glycosidic dihedral angles were used to examine the relative orientation of the sugar and peptide moieties (see Scheme 3). To study the *cis*−*trans* isomerization of the peptide backbone, potential energy surface (PES) scans were carried out using the improper dihedral ζ ($\angle$(CH$_3$−O−C$^{\delta}$−C$^{\alpha}$)) as the reaction coordinate as suggested by Fischer et al.[91] This dihedral is preferred to the peptide ω dihedral as it captures both *cis* and *trans* conformations of the peptide bond, as well as nitrogen pyramidalization, which is an important conformational feature of the *cis*−*trans* isomerization reaction of proline and its derivatives.[64,92] During the scan, ζ in the B3LYP-optimized *trans* isomer was fixed in 10° intervals from 0° to 180°, while the rest of the molecule was allowed to relax. Subsequently, unrestrained optimizations and frequency calculations of stationary points were performed at the same level of theory. All B3LYP calculations employed the IEF−PCM implicit solvation model[93] with ε = 78.39 to represent the water environment and the default parameters in the Gaussian 09 software.[94]

Structural Analysis. The Westhof−Sundaralingam equations[95] were used to analyze the conformation of the five-membered proline ring according to

$$P = \tan^{-1}\left(\frac{B}{A}\right) \quad \text{and} \quad \chi_m = (A^2 + B^2)^{1/2}$$

with

$$A = \frac{2}{5}\sum_{i=1}^{5}\chi_i \cos\left(\frac{4\pi}{5}(i-2)\right) \quad \text{and}$$

$$B = -\frac{2}{5}\sum_{i=1}^{5}\chi_i \sin\left(\frac{4\pi}{5}(i-2)\right)$$

dx.doi.org/10.1021/jp207479q | *J. Phys. Chem. B* 2012, 116, 860–871

Table 1. Pseudorotation Parameters and Glycosidic Dihedral Angles (deg) from MD Simulations and PCM−B3LYP/6-311++G(d,p)[a]

	minimum 1[b]								minimum 2[b,c]							
	B3LYP				MD[d]				B3LYP				MD[d]			
compd	P	χ_m	ϕ_g	ψ_g	P	χ_m	ϕ_g	ψ_g	P	χ_m	ϕ_g	ψ_g	P	χ_m	ϕ_g	ψ_g
Hyp	10	37			12(19)	34(7)										
Hyp−α−Gal	12	37	81	260	10(17)	35(7)	78(14)	267(19)	11	37	74	198	10(17)	35(7)	78(14)	202(15)
Hyp−β−Gal	10	37	284	212	12(16)	35(7)	280(20)	196(27)	12	37	282	274	12(16)	35(7)	280(20)	271(17)
hyp	173	34			178(18)	32(6)			192	37						
hyp−α−Gal	178	34	83	155	177(18)	33(7)	78(13)	156(12)	195	34	75	83	177(18)	33(7)	78(13)	88(14)
hyp−β−Gal	173	34	284	98	178(18)	33(7)	277(30)	85(16)	182	37	284	178	178(18)	33(7)	277(30)	162(16)

[a] See Scheme 3 and the Computational Details for definition of parameters. [b] See Figures 1, 4, and 5 for structures of minima 1 and 2. [c] For unglycosylated hyp, minimum 2 refers to the conformation with an intramolecular hydrogen bond between the C^{γ}-hydroxyl and the peptide backbone. In glycosylated hyp compounds, minimum 2 has an intramolecular hydrogen bond between the sugar and the peptide. [d] Numbers in parentheses refer to the standard deviations.

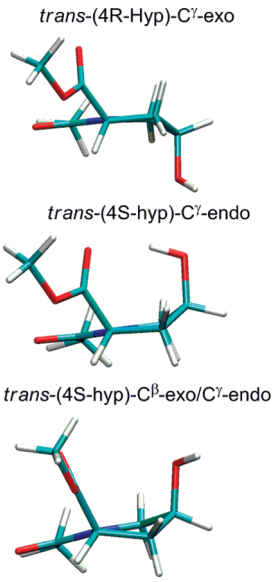

Figure 1. Preferred puckering states of (unglycosylated) 4-hydroxyproline compounds.

where P (pseudorotation phase angle) defines the ring puckering according to the pseudorotation circle and χ_m (pseudorotation amplitude) is the maximum amplitude adopted by any endocyclic torsion angle (χ_i, Scheme 3). Estimates of the conformational free energy differences between minima from MD simulations were obtained using

$$\Delta G_{12} = -K_b T \ln\left(\frac{\%\text{minima 1}}{\%\text{minima 2}}\right)$$

The presence of hydrogen bonds was analyzed based on a distance of less than 3.0 Å between the donor and acceptor, and a donor oxygen, donor hydrogen and acceptor bond angle greater than 120°.

RESULTS AND DISCUSSION

Proline Puckering. The relative orientation of the pyrrolidine and galactose rings is in part dictated by the direction of glycan projection, which is determined by the puckering preference of the hydroxyproline ring. Although different puckering states are predominantly populated by the Hyp and hyp proline derivatives,[96] experimental data has shown that the ring puckering is not substantially affected by glycosylation,[96] and therefore different proline−sugar orientations may prevail for the two stereoisomers. Table 1 displays the average and standard deviation (in parentheses) of the pseudorotation parameters for minima of all compounds (discussed in detail below) obtained from MD simulations, which were calculated using all snapshots in the trajectory, as well as from DFT (PCM−B3LYP/6-311++G(d,p)). In accordance with previous experimental and computational studies,[62,64] both types of calculations predict a C^{γ}-exo ($^{\gamma}$E) envelope-type puckering with a pseudorotation phase angle of $P \approx 10°$ for Hyp (Figure 1, top) and glycosylated Hyp. In contrast, some conformers of the hyp stereoisomer contain a hydrogen bond to the peptide backbone carbonyl oxygen (described in more detail below), which leads to C^{γ}-endo ($_{\gamma}$E) puckering (Figure 1, middle) with $P \approx 200°$ (minimum 2, Table 1). However, in explicit water, there is competition between the C-terminal carbonyl and water molecules for hydrogen bonding. Therefore, the average P values obtained from MD indicate that the proline ring predominantly adopts a twisted C^{γ}-endo/C^{β}-exo ($_{\gamma}T^{\beta}$) conformation with $P \approx 180°$ (Figure 1, bottom; minimum 1, Table 1). These variations in puckering preference of Hyp and hyp will project a covalently attached glycan in different directions relative to the plane of the pyrrolidine ring. Specifically, the $^{\gamma}$E pucker directs C^{γ} below the plane defined by C^{δ}, N, C^{α}, and C^{β} away from O1 (Figure 1 and Scheme 3), while the $_{\gamma}T^{\beta}$ and $_{\gamma}$E puckers direct C^{γ} in the opposite direction.

Relative Orientation of Proline and Sugar Rings. In this section, we more carefully examine the arrangement of the sugar moiety with respect to the peptide. Since the sugar only occupies the preferred $^4C_1$ conformation for the duration of the MD calculations, this conformation was considered in DFT optimizations. Additionally, the ω_g dihedral angle was set to the most stable g^t conformation obtained from MD and the other exocyclic dihedrals in an anticlockwise arrangement. While the general direction of the glycan projection is determined by ring puckering, the preferred values of the ϕ_g and ψ_g glycosidic linkage dihedral angles (Scheme 3, left) control whether interactions

dx.doi.org/10.1021/jp207479q | J. Phys. Chem. B 2012, 116, 860–871

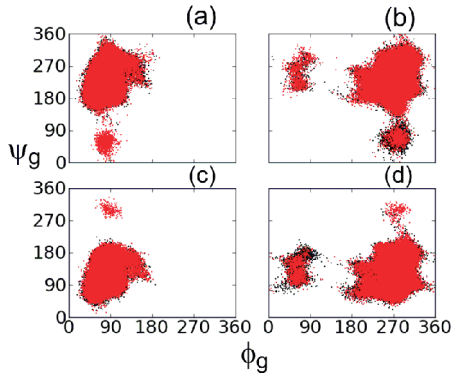

Figure 2. Distribution of glycosidic linkage ϕ_g and ψ_g dihedral angles (deg) obtained from the MD trajectory of the *trans* (black) and *cis* (red) isomers of (a) Hyp−α−Gal, (b) Hyp−β−Gal, (c) hyp−α−Gal, and (d) hyp−β−Gal.

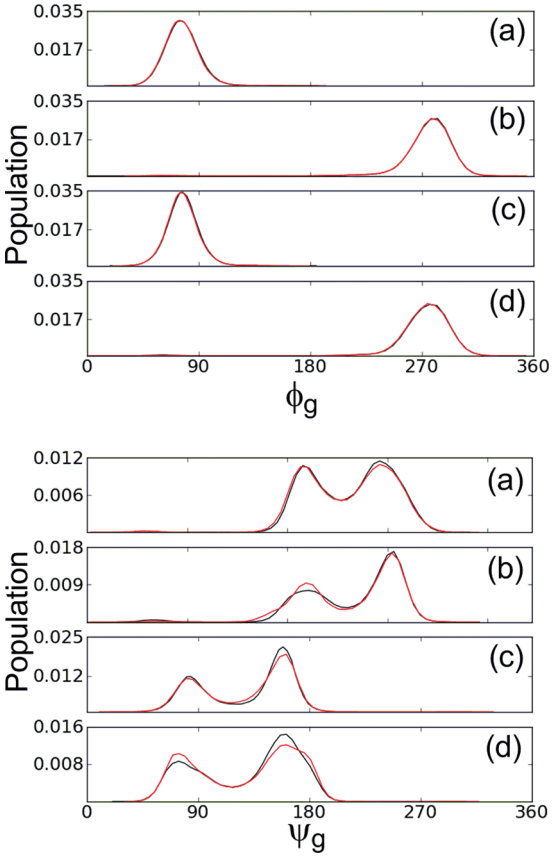

Figure 3. Histograms of the ϕ_g (top) and ψ_g (bottom) glycosidic linkage dihedral angles (deg) obtained from the MD trajectory of the *trans* (black) and *cis* (red) isomers of (a) Hyp−α−Gal, (b) Hyp−β−Gal, (c) hyp−α−Gal, and (d) hyp−β−Gal.

occur between the backbone and sugar moiety. As illustrated by the scatter plots in Figure 2, in combination with the histograms in Figure 3, all glycosylated compounds occupy a single major minimum with respect to ϕ_g, while two major minima exist with respect to ψ_g. This is true for both the *trans* (black) and *cis* (red) conformations. Preliminary DFT scans of these two dihedral angles (data not shown) also confirmed the presence of two

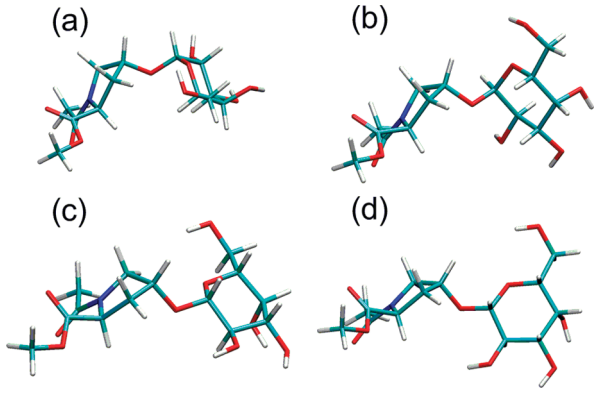

Figure 4. Minima 1 (a,c) and 2 (b,d) with respect to glycosidic linkage dihedral angles ϕ_g and ψ_g of Hyp−α−Gal (a,b) and Hyp−β−Gal (c,d) in the *trans* conformation.

minima for ψ_g. Furthermore, there is very good agreement in the values of the (ϕ_g and ψ_g) dihedrals predicted by molecular mechanics and DFT for all compounds (Table 1). Below, the main (ϕ_g,ψ_g) minima for each glycosylated compound will be individually discussed.

In minimum 1 of Hyp−α−Gal ((ϕ_g,ψ_g) = (81°,260°)), the sugar and Hyp rings are in a near stacked arrangement (Figure 4a). Moreover, the hydrophobic face of the sugar interacts with the peptide, and is thus sheltered from water, which has been observed in crystal structures.[97,98] In minimum 2 (74°,198°), the peptide and sugar rings are more distally arranged (Figure 4b). DFT free energy differences predict that minimum 1 is favored over minimum 2 by approximately 3.4 kJ/mol. Similarly, the estimated free energy from MD simulations suggests minimum 1 is 0.9 kJ/mol more stable than minimum 2. The small free energy differences imply frequent transition between minima, which can also be seen in the evolution of the ψ_g dihedral angle (Figure S1 in the Supporting Information). In fact, several transitions take place in one nanosecond and hence occur on a time scale of a few 100 ps in all glycosylated peptides.

In the two major minima of Hyp−β−Gal (Figure 4, c and d), the sugar and peptide rings are more separated than in the corresponding α-galactosylated peptide. MD free energy estimates indicate that minimum 2 (282°,274°) is favored by approximately 1.3 kJ/mol, while DFT calculations indicate that minimum 1 (284°,212°) is preferred by 1.5 kJ/mol. Nevertheless, these free energy differences are negligible and MD simulations suggest the conversion barrier is small (Figure S1).

As mentioned above, 4S stereochemistry in hyp leads to C^{γ}-endo/C^{β}-exo ($_{\gamma}T^{\beta}$) puckering, which allows the sugar moiety to be pointed in the opposite direction relative to Hyp. Although the rings are more spatially separated than in Hyp−α−Gal due the protrusion of the C-terminal region of the peptide toward the sugar (a consequence of the proline puckering), a stacked-like arrangement of the sugar and peptide moieties prevails in minimum 1 (83°,155°) of hyp−α−Gal (Figure 5a). In minimum 2 (75°,83°), an approximate 70° change in ψ_g brings the C2 hydroxyl of the sugar into hydrogen-bonding contact with the backbone C-terminal carbonyl of the peptide (Figure 5b). DFT calculations predict minimum 2 to be 5.5 kJ/mol more stable due to the intramolecular hydrogen bond, while MD favors minimum 1 by approximately 1.2 kJ/mol. The disparity between DFT and

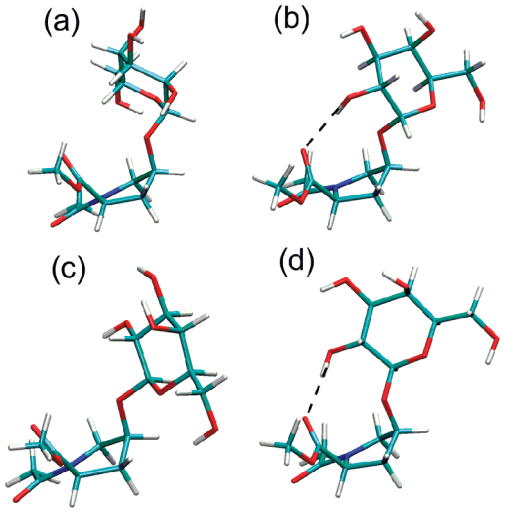

Figure 5. Minima 1 (a,c) and 2 (b,d) with respect to glycosidic linkage dihedral angles ϕ_g and ψ_g of hyp−α−Gal (a,b) and hyp−β−Gal (c,d) in the *trans* conformation. Important intramolecular hydrogen bonds shown with dashed lines.

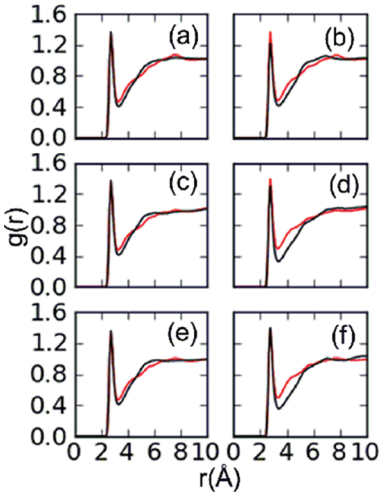

Figure 6. RDFs for interactions between a water oxygen (OW) and O (red) or O1 (black) in the peptide backbone of the *trans* conformation of (a) Hyp, (b) hyp, (c) Hyp−α−Gal, (d) hyp−α−Gal, (e) Hyp−β−Gal, and (f) hyp−β−Gal.

MD may arise due to the lack of explicit water molecules in the QM model or the role of dispersion interactions in the stacked orientation, which may not be fully recovered by B3LYP.[99] However, both types of calculations indicate that the energy difference between the two minima are small and therefore predict two nearly isoenergetic main minima (Figure S1).

As discussed for the 4R-stereoisomer, more extended conformations are observed upon β-glycosylation of hyp compared to the α-glycosylated compound. In minimum 1 (284°,98°), the glycan is directed away from the peptide (Figure 5c), while a hydrogen bond is formed between the sugar C2 hydroxyl group and the C-terminal carbonyl in the peptide backbone in minimum 2 (284°,178°), which creates a 10-membered hydrogen-bonding ring (Figure 5d). Such ring structures are frequently observed in β-turn structures where they stabilize the peptide backbone conformation.[100−102] These geometric differences lead to a DFT (MD) free energy difference of 0.39 (1.21) kJ/mol in favor of minimum 2, and MD suggests frequent transition between these structures (Figure S1).

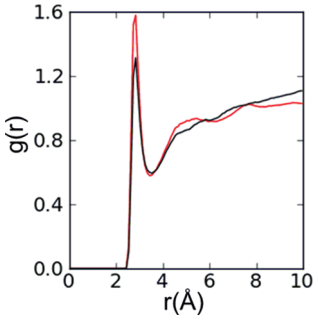

Figure 7. RDFs for interactions between a water oxygen (OW) and O^{δ} in the *trans* conformation of unglycosylated Hyp (red) and hyp (black).

The above results suggest that the relative arrangement of the peptide and sugar rings is jointly determined by the puckering of the proline ring and the glycosidic linkage dihedral angles. 4R glycosylation maintains C^{γ}-exo puckering on the proline ring, while 4S glycosylation primarily induces a twisted C^{γ}-endo/C^{β}-exo ($_{\gamma}T^{\beta}$) ring pucker. These results are fully consistent with previously obtained NMR data.[61] The two puckering states project the glycan onto opposite sides of the plane formed by the proline ring and have different consequences for glycan−peptide interactions. In all compounds considered, the ϕ_g dihedral angle is very rigid ($\phi_g \approx 80°$ for α-linked peptides and $\phi_g \approx 280°$ for β-linked peptides, Figure 2), where the preferred value is mainly determined by the exoanomeric effect. On the other hand, the ψ_g dihedral appears to be governed by the gauche effect with the η ($\angle$(N−C^{δ}−C^{γ}−O^{δ})) dihedral angle adopting values that allow the C^{γ}-substituent to be in a gauche arrangement relative to nitrogen. Thus, by revealing the previously unknown conformation about the hydroxyproline−galactose linkage, our work determines that a combination of factors leads to the most populated proline−sugar conformations.

Solvation and Intramolecular Hydrogen Bonding. Carbohydrates are known to be highly hydrophilic, and therefore formation of glycopeptides can change the local structure of water molecules around the original peptide moiety. Additionally, the previous section showed that the differences in the relative position of the proline and sugar rings upon glycosylation of Hyp and hyp lead to intramolecular hydrogen-bonding interactions, which may affect solvation. These questions are explored in the present section by considering the radial distribution functions (RDFs) and more closely analyzing intramolecular hydrogen-bonding interactions. Since water can hydrogen bond to the N-terminal (O) and C-terminal (O1) carbonyls, as well as the O^{δ} in unglycosylated Hyp and hyp (Scheme 3, right), the RDFs for interactions between these sites and a water oxygen (OW) will be discussed (Figures 6 and 7). The corresponding hydrogen atom (HW) RDFs, as well as all data for the *cis* conformations are provided in the Supporting Information (Figures S2−S7).

For the unglycosylated and glycosylated versions of Hyp, the RDFs involving O (red) and O1 (black) have a clear peak at r = 2.75 Å (Figure 6, left), which confirms the presence of water hydrogen bonding to these sites. The similarity between the RDFs for these two sites for all Hyp derivatives considered here suggests that O and O1 are equally hydrated and stabilized, which is also evidenced by the potential of mean force (PMF) between

dx.doi.org/10.1021/jp207479q |*J. Phys. Chem. B* 2012, 116, 860–871

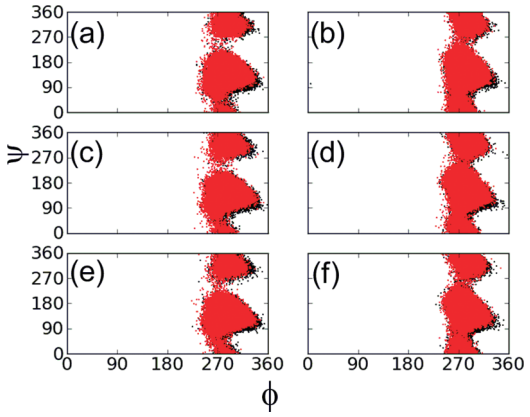

Figure 8. Distributions of peptide backbone ϕ and ψ dihedral angles (deg) in the *trans* (black) and *cis* (red) conformations of (a) Hyp, (b) hyp, (c) Hyp−α−Gal, (d) Hyp−β−Gal, (e) hyp−α−Gal, and (f) hyp−β−Gal.

O or O1 and OW (Figure S7 in the Supporting Information). In unglycosylated Hyp, the O^{δ} site also forms hydrogen-bonding contacts with water (Figure 7). No intramolecular hydrogen bond is detected in any of the Hyp compounds using our geometrical criteria (see Computational Details). Overall, the RDFs indicate that glycosylation does not noticeably alter interactions involving backbone carbonyl groups of Hyp.

In the case of unglycosylated and glycosylated hyp, there is a slightly higher peak in the O (red) than O1 (black) RDFs (Figure 6, right). This suggests that differences exist in the solvation and intramolecular hydrogen-bonding interactions of the N and C-terminal carbonyls, which is also reflected in the PMF plots (Figure S7 in the Supporting Information). In the unglycosylated model, a hydrogen bond exists between O1 and the O^{δ} hydrogen (minimum 2; Figure 1, middle) for a significant amount of time (approximately 32% (24%) of the MD trajectory for the *trans* (*cis*) conformation) even though it is frequently interrupted by surrounding water molecules. This unique interaction in hyp is reflected in a significant reduction in the peak qof the O^{δ}-OW RDF relative to Hyp (Figure 7). Glycosylation of hyp eliminates the O^{δ}-hydroxyl hydrogen and therefore this hydrogen-bonding interaction. Instead, a hydrogen bond forms between O1 and the C2 hydroxyl group of the sugar. This interaction is present in minimum 2 ($(\phi_g,\psi_g) = (75°,83°)$) of the α-glycosylated compound for approximately 12% of the trajectory for the *trans* (8% for *cis*) conformation, and 7% of the trajectory for the *trans* (10% for *cis*) conformation of minimum 2 ($(\phi_g,\psi_g) = (284°,178°)$) of β-glycosylated hyp. Thus, hyp and its glycosylated variants exhibit intramolecular hydrogen bonding in solution between the 4S-substituent and the peptide backbone, which affects backbone hydration. This finding mirrors conclusions previously noted in the literature for hyp and related derivatives[67] but contrasts the lack of intramolecular interactions in Hyp or its galactosylated variants reported in the present work. Additionally, we find that the hydrogen bond can be mediated by a water molecule. Using a simple distance cutoff of 3.5 Å between heavy atoms, the bridged hydrogen bond exists for 16% (22%) of the simulation in the *trans* conformer of $\alpha(\beta)$-glycosylated hyp. This is similar to results in the literature where water bridges have been observed in model glycopeptides.[70,71] The stark contrast between the lack of intramolecular interaction between the peptide backbone and glycan in glycosylated Hyp compounds and the

Table 2. Conformations of the Peptide Backbone (ψ, deg) and PPII Occupation

		B3LYP[b]					
		MD[a]		minimum 1		minimum 2	
compd	% PPII	PPII	α_R	PPII	α_R	PPII	α_R
Hyp	96	131(20)	317(17)	147	323		
Hyp−α−Gal	95	130(20)	317(17)	147	323	147	323
Hyp−β−Gal	94	130(20)	316(17)	146	323	147	323
hyp	94	135(29)	328(20)	175	2	139	321
hyp−α−Gal	83	140(38)	331(18)	171	356	150	329
hyp−β−Gal	90	146(31)	331(19)	173	356	164	351

[a] Data shown are averages over the MD simulation with standard deviations provided in parentheses. [b] PCM−B3LYP/6-311++G(d,p).

interactions found in α/β-glycosylated hyp derivatives may explain the experimentally observed difference in amide isomerization of these derivatives.

Peptide Backbone Conformation. Since glycosylation affects the solvation and intramolecular hydrogen-bonding interactions in hyp, it may also have consequences on the backbone structure; therefore, the conformation of the peptide backbone must be carefully examined. Figure 8 shows Ramachandran plots of the backbone ϕ and ψ dihedral angles (Scheme 3) obtained from MD simulations for the *trans* (black) and *cis* (red) conformations of all compounds. There are two main minima on the PES of the peptide in (ϕ,ψ) space, where the ϕ dihedral remains at approximately 300° for the duration of the simulation, while ψ adopts two values. Specifically, the most populated minimum is a polyproline II-like (PPII) conformation ($(\phi,\psi) \approx (300°,130°)$), while the second minimum is a right-handed α-helix-like (α_R) conformation ($(\phi,\psi) \approx (300°,330°)$).

Hyp exists in the PPII conformation for 96% of the simulation, while Hyp−α−Gal and Hyp−β−Gal adopt this conformation for 95% and 94%, respectively (Table 2). Furthermore, there is almost no difference in the average values of the backbone dihedral angles in all Hyp compounds, which is supported by DFT-optimized structures (Table 3). Therefore, glycosylation of Hyp does not change the preferred conformation of the peptide backbone. This is not surprising since glycosylation does not lead to new intramolecular interactions.

In contrast to Hyp, there are significant changes in the peptide backbone upon glycosylation of hyp (Tables 2 and 3). First, there is an increase in the α_R population, where the PPII population decreases from 94% in hyp to 83% (90%) in the $\alpha(\beta)$-glycosylated version (Table 2). In DFT-optimized α_R conformations (Figure S8 in the Supporting Information), contacts exist between the peptide methoxyl group at C1 and the C2 hydroxyl group of the sugar in both glycosylated versions of hyp, which may provide further stabilization to the α_R structure for these derivatives compared to glycosylated Hyp. Second, there are differences in the average values of important backbone dihedral angles in the PPII conformation of unglycosylated and glycosylated hyp. In particular, ψ from MD simulations averages 135° in hyp, but 140° and 146° in hyp−α−Gal and hyp−β−Gal, respectively. DFT results in this work (Table 3), as well as other studies,[62,67] reveal that in the absence of a hydrogen bond between the C^{γ}−OH group and the C-terminal backbone

Table 3. PCM−B3LYP/6-311++G(d,p) Structural Parameters at Stationary Points of Hyp and hyp Compounds

	minimum 1[a]								minimum 2[a,b]							
compd	ϕ[c]	ψ[c]	ξ[d]	ω[c]	ρ[e]	P	χ_m	η[f]	ϕ[c]	ψ[c]	ξ[d]	ω[c]	ρ[e]	P	χ_m	η[f]
Hyp																
trans	299	147	179	182	356	10	37	86								
TS	281	167	84	116	328	−33	41									
cis	292	160	357	1	355	17	37									
Hyp−α−Gal																
trans	298	147	179	182	356	12	37	83	298	147	179	183	356	11	37	85
TS	286	167	83	117	324	264	45		279	167	85	116	328	−28	41	
cis	292	160	357	0	356	18	37		291	161	357	2	355	19	37	
Hyp−β−Gal																
trans	299	146	179	183	356	10	37	83	298	147	179	183	357	12	37	85
TS	279	166	84	116	328	−31	41		281	166	84	116	327	−37	41	
cis	292	161	357	1	4	18	37		292	161	357	1	356	18	37	
hyp																
trans	282	175	179	183	359	173	34	266	294	139	183	183	1	192	37	272
TS	268	77	81	114	326	229	40		254	117	115	84		203	39	
cis	278	184	359	1	357	165	36		281	139	1	5	1	180	35	
hyp−α−Gal																
trans	283	171	179	183	355	178	34	270	294	150	180	183	356	195	34	273
TS	286	169	83	117	324	263	45		260	84	84	115	327	215	39	
cis	279	178	359	2	356	169	36		282	166	0	4	355	178	36	
hyp−β−Gal																
trans	282	173	180	183	356	173	34	266	286	164	180	183	357	182	37	278
TS	285	169	83	117	324	263	45		253	166	85	116	329	201	41	
cis	278	182	359	2	357	166	36		280	173	0	3	356	174	38	

[a] See Figures 1, 4, and 5 for structures of minima 1 and 2. [b] For unglycosylated hyp, minimum 2 refers to the conformation with an intramolecular hydrogen bond between the C^{γ}-hydroxyl and the peptide backbone. In glycosylated hyp compounds, minimum 2 has an intramolecular hydrogen bond between the sugar and the peptide. [c] Peptide backbone dihedral angles defined in Scheme 2. [d] ξ is the $\angle(CH_3-O-C^{\delta}-C^{\alpha})$ improper dihedral angle (see Scheme 3). [e] ρ is the $\angle(N-C-C^{\alpha}-C^{\delta})$ improper dihedral angle. [f] η is the $\angle(N-C^{\delta}-C^{\gamma}-O^{\delta})$ dihedral angle.

carbonyl oxygen in hyp (minimum 1; Figure 1, bottom), the ψ dihedral angle is close to 180°. However, in the presence of this hydrogen bond (minimum 2; Figure 1, middle), which provides stabilization to the overall structure, ψ adopts a value of approximately 140°. Upon glycosylation of hyp, both MD and DFT predict ψ values closer to 180° (minimum 2), while at the same time the structure maintains stability via intramolecular hydrogen bonding.

In summary, glycosylation of Hyp does not affect the peptide backbone in accordance with experimental findings.[61,103] However, glycosylation of hyp allows the ψ dihedral angle to relax to larger values and, therefore, induces changes to the backbone of hyp. Since this feature, coupled with the intramolecular hydrogen-bonding interactions discussed previously, is the main structural difference between glycosylated Hyp and hyp, it may be the reason for increased *trans* stabilization upon glycosylation of hyp. Hence, the details of the *cis*/*trans* isomerization will be considered in the next section.

Prolyl Amide Isomerization. We first discuss the peptide backbone structure at various stationary points on the PES for *cis*/*trans* isomerization (Table 3). For unglycosylated and glycosylated Hyp compounds, ϕ is approximately 300° for the *trans* and *cis* isomers, and decreases by ∼20° in the transition state (TS). The ψ dihedral angle approximately equals 147° in the *trans* conformation and shifts to ∼167° in the TS and 160° in the *cis* conformation. Although the ζ and ω dihedral angles remain at 0° in the *cis* and 180° in the *trans* isomer, ζ and ω become ∼84° and 116° in the TS, respectively. An interesting known feature of *cis*−*trans* conversion in proline and its derivatives is the pyramidalization of the nitrogen atom, which leads to a tetrahedral structure in the TS.[64] This feature is well reproduced in our calculations, where ρ (the improper dihedral that measures this pyramidalization) decreases from ∼355° in both the *trans* and *cis* conformations to 325° in the TS. This pyramidalization changes the pyrrolidine ring conformation (P changes from ∼10° to 30° and χ_m increases from 37° to over 40°). Overall, these important geometric features are very similar in unglycosylated and glycosylated Hyp regardless of the conformation adopted by the glycosylated derivative, which suggests that glycosylation does not affect the structures of the stationary points involved in the Hyp isomerization reaction.

Figure 9 plots the PCM−B3LYP/6-311++G(d,p) energy as a function of the ζ ($\angle(CH_3-O-C^{\delta}-C^{\alpha})$, Scheme 3) dihedral angle, while thermodynamic parameters for the *cis*−*trans* isomerization of Hyp compounds are given in Table 4 and the corresponding activation parameters are in Table S1 in the Supporting Information. All calculated activation enthalpies are approximately 83 kJ/mol, which is in line with other theoretical[63,64] and experimental[64] studies for Hyp. Similarly, computed activation free energies are approximately 84−86 kJ/mol in accordance

dx.doi.org/10.1021/jp207479q | J. Phys. Chem. B 2012, 116, 860–871

with previous modeling studies of related compounds.[63] There are no significant differences in the thermodynamic and activation data for the unglycosylated and glycosylated Hyp compounds, which suggests that glycosylation does not affect isomerization. The good agreement between calculated and experimental data (Table 4) indicates that our methodology adequately describes this isomerization process.

In the absence of a hydrogen bond to the peptide backbone in hyp (minimum 1), the ϕ dihedral angle assumes a value of approximately 282° in the *trans* isomer (Table 2). If a hydrogen bond to the backbone exists (minimum 2), then ϕ becomes 294° in hyp and hyp−α−Gal, and 286° in hyp−β−Gal. This shows that intramolecular hydrogen bonding affects the ϕ dihedral angle, where the preferred value becomes more similar to that in Hyp. In the *trans*, TS, and *cis* conformations of 4S-hyp, ζ is approximately 180°, 84°, and 0°, while ω is approximately 180°, 115°, and 0°, respectively, in both minima. In minimum 1 for the *trans* isomer of all hyp compounds, ψ is 171−175°. However, there is a significant change in the ψ dihedral upon hydrogen-bond formation (minimum 2). Specifically, ψ decreases to 139° in hyp, 150° in hyp−α−Gal, and 165° in hyp−β−Gal. Hence, hydrogen bonding to the peptide backbone in hyp has a significant impact on the structure of the peptide, which could affect isomerization upon glycosylation.

The calculated free energy and enthalpy values for the non-hydrogen-bonded conformation of hyp (minimum 1) are closer to the experimental values than those for the hydrogen-bonded conformation (minimum 2). Using our distance and angle cutoffs, molecular dynamics calculations indicate that the hydrogen bond exists in unglycosylated hyp for only approximately one-third of the simulation time in solution. In contrast, DFT calculations in implicit solvation suggest that the hydrogen-bonded conformation is slightly preferred, but the associated $\Delta S_{cis-trans}$ has the opposite sign compared to experiment. Thus, it is likely that the lack of explicit water molecules in DFT calculations is responsible for the stability preference of the hydrogen-bonded conformation. Therefore, although hyp can adopt both reported conformations, the non-hydrogen-bonded conformation likely prevails in solution, which is supported by similar $K_{trans/cis}$ measured when the C^{γ}-hydroxyl group in hyp is replaced by fluorine.[53] This again shows the need for including explicit water molecules in the calculations.

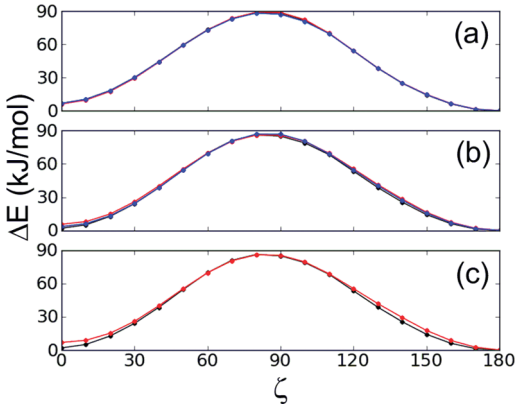

Figure 9. PCM−B3LYP/6-311++G(d,p) scans of the energy as a function of the ζ improper dihedral angle (deg) describing *cis*−*trans* isomerization in (a) Hyp (black), Hyp−α−Gal (red), and Hyp−β−Gal (blue); (b) hyp (black), hyp−α−Gal (red), and hyp−β−Gal (blue); and (c) hyp with (red) and without (black) an intramolecular hydrogen bond.

Despite the lack of complete agreement between the calculated and experimental thermodynamic parameters (Table 4), structural information suggests that the observed changes in the *trans* to *cis* ratio and isomerization rate upon glycosylation of hyp are likely due to changes in intramolecular hydrogen bonding. Specifically, the *cis*/*trans* isomerization of proline and derivatives is mostly governed by an $n \rightarrow \pi^*$ interaction between the N-terminal amide carbonyl O and C-terminal carbonyl C bond, which requires $\psi \approx 150°$.[50,104,105] Changes to ψ upon glycosylation due to changes in intramolecular hydrogen bonding could alter this interaction and thereby lead to a more favorable *trans* conformation. In Hyp compounds, glycosylation has no effect on the isomerization since the C^{γ}-exo puckering orients the sugar away from the peptide backbone, which prevents formation of intramolecular interactions that alter ψ and the $n \rightarrow \pi^*$ interaction. However, several intramolecular hydrogen-bonding interactions involving the peptide backbone occur in hyp and glycosylated compounds, and the discussion below explains how these affect the geometry about ψ, the $n \rightarrow \pi^*$ interaction, and the experimentally measured *cis*/*trans* ratios.

Our work emphasizes that there are two main minima of unglycosylated hyp (Table 3, Figure 1), where the structure with a strong hydrogen bond between 4-OH and the peptide backbone is present for one-third of the MD calculation. Although the effect of the structure with the intramolecular hydrogen bond on the isomerization process in water is not completely understood, experimental studies suggest that it is of little consequence. Specifically, the $K_{trans/cis}$ measured for hyp (2.7) is similar to that for O-methylated hyp (2.0), which does not contain an intramolecular hydrogen bond to the backbone.[66] Similarly, another study reports a $K_{trans/cis}$ of 2.4 for hyp versus 2.5 for

Table 4. Calculated Thermodynamic Parameters for *Cis*−*Trans* Isomerization in hyp and Hyp Compounds in Comparison to Experimental Data[a]

	minimum 1[b]				minimum 2[b]				experiment[c]		
compd	ΔH	ΔE	ΔS	ΔG	ΔH	ΔE	ΔS	ΔG	ΔH	ΔS	ΔG
Hyp	−6.20	−5.93	−5.61	−4.52					−5.98(0.17)	−4.89(0.46)	−4.52(0.29)
Hyp−α−Gal	−6.28	−6.11	−8.28	−3.82	−5.65	−5.40	−7.03	−3.56	−5.94(0.50)	−4.77(1.55)	−4.52(0.96)
Hyp−β−Gal	−5.50	−6.17	−6.35	−3.61	−5.87	−5.23	−12.55	−2.12	−6.06(0.54)	−5.77(1.71)	−4.35(1.04)
hyp	−2.03	−2.29	4.31	−3.31	−6.95	−6.90	−3.81	−5.82	−1.21(0.33)	3.31(1.05)	−2.22(0.67)
hyp−α−Gal	−2.29	−2.16	−3.56	−1.22	−5.28	−5.06	−0.96	−4.99	−3.92(0.54)	−4.31(1.76)	−2.64(1.09)
hyp−β−Gal	−1.82	−2.01	5.31	−3.40	−3.31	−3.17	−1.63	−2.82	−3.81(0.21)	−4.02(0.67)	−2.59(0.42)

[a] ΔH, ΔE, and ΔG are in kJ/mol, while ΔS is in J/(mol K). See Figures 2, 5, and 6. [b] PCM−B3LYP/6-311++G(d,p). [c] From ref 90.

dx.doi.org/10.1021/jp207479q | J. Phys. Chem. B 2012, 116, 860–871

4S-fluoroproline.[50] Furthermore, since the hydrogen-bonded conformation of unglycosylated hyp has a ψ dihedral angle (~140°) appropriate for the n → π^* interaction, the dominance of this conformation should lead to an increased *trans* conformation, which is in contrast to experimental observations. Thus, when the solvent competes for hydrogen-bonding interactions with 4-OH, the measured $K_{trans/cis}$ suggest that hyp preferentially adopts the non-hydrogen-bonded conformation to maximize the solute−solvent interactions. We note that, although the hydrogen-bonded conformation is likely not prevalent in water, it may become more important in non-hydrogen-bonding solvents. Indeed, $K_{trans/cis}$ of unglycosylated hyp increases to 5.0 in $CDCl_3$.[66]

The above discussion suggests that the non-hydrogen-bonded conformation of hyp (minimum 2) is dominant in water, and therefore the removal of the 4-OH to backbone hydrogen bond cannot explain the experimentally measured changes in the *cis*/*trans* ratio upon glycosylation. Instead, it is the creation of new hydrogen-bonding interactions upon glycosylation that is responsible for the observed changes. Specifically, our calculations show that, in the more prevalent non-hydrogen-bonded conformation of hyp, the ψ dihedral is approximately 180° and the favorable n → π^* interaction is largely absent. For comparison, a similar conformation about ψ occurs in the DFT-optimized minimum of O-methylated hyp (Figure S10 in the Supporting Information), which cannot form an intramolecular hydrogen bond with the peptide backbone. However, upon $\alpha(\beta)$-galactosylation of hyp, the ψ dihedral adopts a value of 150°(164°) in the hydrogen-bonded structure (minimum 2), which strengthens the n → π^* interaction and leads to the observed increase in the population of the *trans* isomer.

To provide further support for the above analysis, interaction energies were estimated with second-order perturbation theory using natural bond orbital (NBO) calculations. Models of the glycosylated compounds in implicit water, as well as in the gas phase with 10 explicit water molecules that represent the first few solvation shells about O1 (and include the bridging water, Figures S11 and S12 in the Supporting Information), were considered. NBO calculations on the PCM−B3LYP/6-311++G(d,p) optimized structure of hyp−α−Gal indicate that the n → π^* interaction stabilizes the *trans* conformation by approximately 3 kJ/mol. However, this favorable interaction is largely absent in the β-glycosylated model. When 10 water molecules were included in the B3LYP/6-31G(d) optimization, NBO calculations reveal that the *trans* conformation in the $\alpha(\beta)$-glycosylated hyp is stabilized by approximately 12(4) kJ/mol. For comparison, similar calculations show that essentially zero stabilization is gained in the non-hydrogen-bonded conformation of unglycosylated hyp, as well as 4-O-methyl hyp, in the gas phase or implicit solvent. Therefore, these calculations support our new proposal that glycosylation turns on the n → π^* interaction that is absent in the dominant conformation of unglycosylated hyp, and leads to the increased *trans* population observed in experiments.[61]

In summary, glycosylation does not significantly change the structure of Hyp and hence does not affect amide isomerization in this proline derivative. This is further supported by the good agreement between calculated and experimental thermodynamic data. However, intramolecular hydrogen-bonding interactions occur between the backbone of hyp and glycan OH groups. These interactions change the structure of the peptide backbone, which likely leads to the experimentally observed differences in amide isomerization.

CONCLUSIONS

This work provides the first molecular level information about the nature of the hydroxyproline−galactose linkage that is prevalent in the hydroxyproline-rich glycoproteins of plants, as well as explains the effects of glycosylation on amide isomerization of 4*R*(*S*)-hydroxyproline. Extensive MD calculations using the AMBER/GLYCAM force field in explicit solvent and complementary (implicit solvent) PCM−B3LYP/6-311++G(d,p) geometry optimizations were used to examine the conformation of the (glyco)peptides. Both methods show that all glycosylated compounds exhibit two main minima with respect to the glycosidic linkage. Since (unglycosylated) Hyp adopts C^{γ}-exo puckering, the sugar molecule is orientated away from the peptide backbone, and glycosylation has no apparent effect. This explains experimental studies that indicate there is no change in the peptide isomerization upon glycosylation. In contrast, a twisted C^{γ}-endo/C^{β}-exo ($_{\gamma}T^{\beta}$) puckering state is dominant in hyp, which brings the sugar and the proline rings in close proximity and leads to hydrogen-bonding interactions between the C2 hydroxyl group of the sugar and the peptide backbone C-terminal carbonyl that is sometimes mediated by a water molecule. Our data indicates that this hydrogen bond affects the structure of the peptide backbone and is likely responsible for the experimentally observed increase in the *trans* conformation population. Therefore, in addition to affording information on the effects of glycosylation on the Hyp backbone, we provide the first explanation for the experimentally measured increase in *trans* isomer population in hyp upon glycosylation. In addition, our study provides evidence for a 10-membered intramolecular hydrogen-bonding ring between a sugar hydroxyl group and the peptide carbonyl group in hyp−α−Gal and hyp−β−Gal that affects N-terminal prolyl amide *cis*/*trans* isomerization. The data presented here may provide the basis to design novel proline probes to control *cis*/*trans* isomerizaton in peptides. Moreover, our study provides new insight into how the projection of a glycan from the peptide or protein backbone exerts its influence on kinetics and thermodynamics of prolyl amide *cis*/*trans* isomerization. Current studies are underway to examine larger oligopeptides, as well as incorporate polysaccharides, in attempts to elucidate the functions of carbohydrates in HRGPs.

ASSOCIATED CONTENT

Supporting Information. Table with activation parameters for *cis*−*trans* isomerization, RDFs for various water interaction sites in all compounds, PCM−B3LYP/6-311++G(d,p) structures for α_R conformation in glycosylated Hyp and hyp, and plots of the evolution of the glycosidic linkage as well as peptide backbone dihedral angles during MD simulations. This material is available free of charge via the Internet at http://pubs.acs.org.

AUTHOR INFORMATION

Corresponding Author

*E-mail: stacey.wetmore@uleth.ca. Phone: 403-329-2323. Fax: 403-329-2057.

ACKNOWLEDGMENT

This research was supported by the Natural Sciences and Engineering Research Council of Canada (NSERC), the Canada Foundation for Innovation (CFI), the Canada Research Chair

(CRC) program, and the University of Lethbridge. Calculations were conducted using resources available through the Western Canada Research Grid (WestGrid and Compute/Cacul Canada) and the Upscale and Robust Abacus for Chemistry In Lethbridge (URACIL).

REFERENCES

(1) Messner, P. *J. Bacteriol.* **2004**, *186*, 2517–2519.
(2) Eichler, J.; Adams, M. W. W. *Microbiol. Mol. Biol. Rev.* **2005**, *69*, 393–425.
(3) Weerepana, E.; Imperiali, B. *Glycobiology* **2006**, *16*, 91R–101R.
(4) Varki, A. *Glycobiology* **1993**, *3*, 97–130.
(5) Dwek, R. A. *Chem. Rev. (Washington, D. C.)* **1996**, *96*, 683–720.
(6) Reuter, G.; Gabius, H. J. *Cell. Mol. Life Sci.* **1999**, *55*, 368–422.
(7) Petrescu, A. J.; Petrescu, S. M.; Dwek, R. A.; Wormald, M. R. *Glycobiology* **1999**, *9*, 343–352.
(8) Mer, G.; Hietter, H.; Lefevre, J.-F. *Nat. Struct. Biol.* **1996**, *3*, 45–53.
(9) Imperiali, B.; Rickert, K. W. *Proc. Natl. Acad. Sci. U.S.A.* **1995**, *92*, 97–101.
(10) Fisher, J. F.; Harrison, A. W.; Bundy, G. L.; Wilkinson, K. F.; Rush, B. D.; Ruwart, M. J. *J. Med. Chem.* **1991**, *34*, 3140–3143.
(11) Mehta, S.; Meldal, M.; Duus, J. O.; Bock, K. *J. Chem. Soc., Perkin Trans. 1* **1999**, 1445–1452.
(12) Imperiali, B. *Acc. Chem. Res.* **1997**, *30*, 452–459.
(13) Bilsky, E. J.; Egleton, R. D.; Mitchell, S. A.; Palian, M. M.; Davis, P.; Huber, J. D.; Jones, H.; Yamamura, H. I.; Janders, J.; Davis, T. P.; Porreca, F.; Hruby, V. J.; Polt, R. *J. Med. Chem.* **2000**, *43*, 2586–2590.
(14) Specker, D.; Wittmann, V. *Top. Curr. Chem.* **2007**, *267*, 65–107.
(15) Meyer, B.; Moeller, H. *Top. Curr. Chem.* **2007**, *267*, 187–251.
(16) Bosques, C. J.; Tschampel, S. M.; Woods, R. J.; Imperiali, B. *J. Am. Chem. Soc.* **2004**, *126*, 8421–8425.
(17) O'Connor, S. E.; Imperiali, B. *Chem. Biol.* **1998**, *5*, 427–437.
(18) Pao, Y.-L.; Wormarld, M. R.; Dwek, R. A.; Lellouch, A. C. *Biochem. Biophys. Res. Commun.* **1996**, *219*, 157–162.
(19) Liang, R.; Andreotti, A. H.; Kahne, D. *J. Am. Chem. Soc.* **1995**, *117*, 10395–10396.
(20) Varki, A. *Glycobiology* **1993**, *3*, 97–130.
(21) Kieliszewski, M. J.; Lamport, D. T. A.; Tan, L.; Cannon, M. C. *Annu. Plant Rev.* **2011**, *41*, 321–342.
(22) Lamport, D. T. A. *Nature (London)* **1967**, *216*, 1322–1324.
(23) Lamport, D. T. A. *Recent Adv. Phytochem.* **1977**, *11*, 79–115.
(24) Knox, R. B.; Clarke, A.; Harrison, S.; Smith, P.; Marchalonis, J. J. *Proc. Natl. Acad. Sci. U.S.A.* **1976**, *73*, 2788–2792.
(25) Showalter, A. M. *Plant Cell* **1993**, *5*, 9–23.
(26) Bowles, D. J. *Annu. Rev. Biochem.* **1990**, *59*, 873–907.
(27) Jose-Estanyol, M.; Puigdomenech, P. *Plant Physiol. Biochem. (Paris)* **2000**, *38*, 97–108.
(28) Sommer-Knudsen, J.; Bacic, A.; Clarke, A. E. *Phytochemistry* **1998**, *47*, 483–497.
(29) Kieliszewski, M. J. *Phytochemistry* **2001**, *57*, 319–323.
(30) Khashimova, Z. S. *Chem. Nat. Compd.* **2003**, *39*, 229–236.
(31) Owens, N. W.; Stetefeld, J.; Lattova, E.; Schweizer, F. *J. Am. Chem. Soc.* **2010**, *132*, 5036–5042.
(32) Mauger, A. B. *J. Nat. Prod.* **1996**, *59*, 1205–1211.
(33) Brandts, J. F.; Halvorson, H. R.; Brennan, M. *Biochemistry* **1975**, *14*, 4953–4963.
(34) MacArthur, M. W.; Thornton, J. M. *J. Mol. Biol.* **1991**, *218*, 397–412.
(35) Stein, R. L. *Adv. Protein Chem.* **1993**, *44*, 1–24.
(36) Fischer, G.; Schmid, F. X. *Biochemistry* **1990**, *29*, 2205–2212.
(37) Sapse, A. M.; Mallah-Levy, L.; Daniels, S. B.; Erickson, B. W. *J. Am. Chem. Soc.* **1987**, *109*, 3526–3529.
(38) Tanaka, S.; Scheraga, H. A. *Macromolecules* **1974**, *7*, 698–705.
(39) Rose, G. D.; Gierasch, L. M.; Smith, J. A. *Adv. Protein Chem.* **1985**, *37*, 1–109.
(40) Halab, L.; Gosselin, F.; Lubell, W. D. *Biopolymers* **2000**, *55*, 101–122.
(41) Halab, L.; Lubell, W. D. *J. Am. Chem. Soc.* **2002**, *124*, 2474–2484.
(42) Kakinoki, S.; Hirano, Y.; Oka, M. *Polym. Bull. (Heidelberg, Ger.)* **2005**, *53*, 109–115.
(43) Berg, R. A.; Prockop, D. J. *Biochem. Biophys. Res. Commun.* **1973**, *52*, 115–120.
(44) Persikov, A. V.; Ramshaw, J. A. M.; Kirkpatrick, A.; Brodsky, B. *Biochemistry* **2000**, *39*, 14960–14967.
(45) Vanholst, G. J.; Varner, J. E. *Plant Physiol.* **1984**, *74*, 247–251.
(46) Shpak, E.; Barbar, E.; Leykam, J. F.; Kieliszewski, M. J. *J. Biol. Chem.* **2001**, *276*, 11272–11278.
(47) Ferris, P. J.; Waffenschmidt, S.; Umen, J. G.; Lin, H.; Lee, J.-H.; Ishida, K.; Kubo, T.; Lau, J.; Goodenough, U. W. *Plant Cell* **2005**, *17*, 597–615.
(48) Zimmerman, S. S.; Scheraga, H. A. *Macromolecules* **1976**, *9*, 408–416.
(49) Zimmerman, S. S.; Scheraga, H. A. *Biopolymers* **1977**, *16*, 811–843.
(50) Bretscher, L. E.; Jenkins, C. L.; Taylor, K. M.; DeRider, M. L.; Raines, R. T. *J. Am. Chem. Soc.* **2001**, *123*, 777–778.
(51) Hodges, J. A.; Raines, R. T. *Org. Lett.* **2006**, *8*, 4695–4697.
(52) Taylor, C. M.; Hardre, R.; Edwards, P. J. B.; Park, J. H. *Org. Lett.* **2003**, *5*, 4413–4416.
(53) Bretscher, L. E.; Jenkins, C. L.; Taylor, K. M.; DeRider, M. L.; Raines, R. T. *J. Am. Chem. Soc.* **2001**, *123*, 777–778.
(54) Eberhardt, E. S.; Panisik, N., Jr.; Raines, R. T. *J. Am. Chem. Soc.* **1996**, *118*, 12261–12266.
(55) DeRider, M. L.; Wilkens, S. J.; Waddell, M. J.; Bretscher, L. E.; Weinhold, F.; Raines, R. T.; Markley, J. L. *J. Am. Chem. Soc.* **2002**, *124*, 2497–2505.
(56) Renner, C.; Alefelder, S.; Bae, J. H.; Budisa, N.; Huber, R.; Moroder, L. *Angew. Chem., Int. Ed.* **2001**, *40*, 923–925.
(57) Cadamuro, S. A.; Reichold, R.; Kusebauch, U.; Musiol, H.-J.; Renner, C.; Tavan, P.; Moroder, L. *Angew. Chem., Int. Ed.* **2008**, *47*, 2143–2146.
(58) Sonntag, L.-S.; Schweizer, S.; Ochsenfeld, C.; Wennemers, H. *J. Am. Chem. Soc.* **2006**, *128*, 14697–14703.
(59) Shoulders, M. D.; Hodges, J. A.; Raines, R. T. *J. Am. Chem. Soc.* **2006**, *128*, 8112–8113.
(60) Owens, N. W.; Braun, C.; O'Neil, J. D.; Marat, K.; Schweizer, F. *J. Am. Chem. Soc.* **2007**, *129*, 11670–11671.
(61) Owens, N. W.; Lee, A.; Marat, K.; Schweizer, F. *Chem.—Eur. J.* **2009**, *15*, 10649–10657.
(62) Improta, R.; Benzi, C.; Barone, V. *J. Am. Chem. Soc.* **2001**, *123*, 12568–12577.
(63) Song, I. K.; Kang, Y. K. *J. Phys. Chem. B* **2006**, *110*, 1915–1927.
(64) Aliev, A. E.; Bhandal, S.; Courtier-Murias, D. *J. Phys. Chem. A* **2009**, *113*, 10858–10865.
(65) Aliev, A. E.; Courtier-Murias, D. *J. Phys. Chem. B* **2007**, *111*, 14034–14042.
(66) Shoulders, M. D.; Kotch, F. W.; Choudhary, A.; Guzei, I. A.; Raines, R. T. *J. Am. Chem. Soc.* **2010**, *132*, 10857–10865.
(67) Kuemin, M.; Nagel, Y. A.; Schweizer, S.; Monnard, F. W. Ochsenfeld, C.; Wennemers, H. *Angew. Chem., Int. Ed.* **2010**, *49*, 6324–6327.
(68) Zhang, K.; Teklebrhan, R. B.; Schreckenbach, G.; Wetmore, S.; Schweizer, F. *J. Org. Chem.* **2009**, *74*, 3735–3743.
(69) Teklebrhan, R. B.; Zhang, K. D.; Schreckenbach, G.; Schweizer, F.; Wetmore, S. D. *J. Phys. Chem. B* **2010**, *114*, 11594–11602.
(70) Corzana, F.; Busto, J. H.; Engelsen, S. B.; Jimenez-Barbero, J.; Asensio, J. L.; Peregrina, J. M.; Avenoza, A. *Chem.—Eur. J.* **2006**, *12*, 7864–7871.
(71) Corzana, F.; Busto, J. H.; Jimenez-Oses, G.; Asensio, J. L.; Jimenez-Barbero, J.; Peregrina, J. M.; Avenoza, A. *J. Am. Chem. Soc.* **2006**, *128*, 14640–14648.
(72) Corzana, F.; Busto, J. H.; Jiménez-Osés, G.; García de Luis, M.; Asensio, J. L.; Jiménez-Barbero, J.; Peregrina, J. M.; Avenoza, A. *J. Am. Chem. Soc.* **2007**, *129*, 9458–9467.

(73) Ali, M. M. N.; Aich, U.; Varghese, B.; Perez, S.; Imberty, A.; Loganathan, D. *J. Am. Chem. Soc.* **2008**, *130*, 8317–8325.
(74) Kirschner, K. N.; Woods, R. J. *Proc. Natl. Acad. Sci. U.S.A.* **2001**, *98*, 10541–10545.
(75) Pearlman, D. A.; Case, D. A.; Caldwell, J. W.; Ross, W. S.; Cheatham, T. E.; Debolt, S.; Ferguson, D.; Seibel, G.; Kollman, P. *Comput. Phys. Commun.* **1995**, *91*, 1–41.
(76) Case, D. A.; Cheatham, T. E.; Darden, T.; Gohlke, H.; Luo, R.; Merz, K. M.; Onufriev, A.; Simmerling, C.; Wang, B.; Woods, R. J. *J. Comput. Chem.* **2005**, *26*, 1668–1688.
(77) Hornak, V.; Abel, R.; Okur, A.; Strockbine, B.; Roitberg, A.; Simmerling, C. *Proteins* **2006**, *65*, 712–725.
(78) Park, S.; Radmer, R. J.; Klein, T. E.; Pande, V. S. *J. Comput. Chem.* **2005**, *26*, 1612–1616.
(79) Kirschner, K. N.; Yongye, A. B.; Tschampel, S. M.; Gonzalez-Outeirino, J.; Daniels, C. R.; Foley, B. L.; Woods, R. J. *J. Comput. Chem.* **2008**, *29*, 622–655.
(80) Cieplak, P.; Cornell, W. D.; Bayly, C.; Kollman, P. A. *J. Comput. Chem.* **1995**, *16*, 1357–1377.
(81) Dupradeau, F.-Y.; Pigache, A.; Zaffran, T.; Savineau, C.; Lelong, R.; Grivel, N.; Lelong, D.; Rosanski, W.; Cieplak, P. *Phys. Chem. Chem. Phys.* **2010**, *12*, 7821–7839.
(82) Clarke, C.; Woods, R. J.; Gluska, J.; Cooper, A.; Nutley, M. A.; Boons, G.-J. *J. Am. Chem. Soc.* **2001**, *123*, 12238–12247.
(83) Ryckaert, J.-P.; Ciccotti, G.; Berendsen, H. J. C. *J. Comput. Phys.* **1977**, *23*, 327–341.
(84) Case, D. A.; Darden, T. A.; Cheatham, III, T. E.; Simmerling, C. L.; Wang, J.; Duke, R. E.; Luo, R.; Crowley, M.; Walker, R. C.; Zhang, W.; Merz, K. M.; Wang, B.; Kollman, P. A.; et al. *AMBER 10*; University of California: San Francisco, 2008.
(85) Momany, F. A.; Willett, J. L.; Schnupf, U. *Theochem—J. Mol. Struct.* **2010**, *953*, 61–82.
(86) Momany, F. A.; Schnupf, U. *Carbohydr. Res.* **2011**, *346*, 619–630.
(87) Momany, F. A.; Appell, M.; Willett, J. L.; Bosma, W. B. *Carbohydr. Res.* **2005**, *340*, 1638–1655.
(88) Momany, F. A.; Appell, M.; Strati, G.; Willett, J. L. *Carbohydr. Res.* **2004**, *339*, 553–567.
(89) Cheeseman, J. R.; Shaik, M. S.; Popelier, P. L. A.; Blanch, E. W. *J. Am. Chem. Soc.* **2011**, *133*, 4991–4997.
(90) French, A. D.; Johnson, G. P.; Kelterer, A.-M.; Dowd, M. K.; Cramer, C. J. *J. Phys. Chem. A* **2002**, *106*, 4988–4997.
(91) Fischer, S.; Dunbrack, R. L.; Karplus, M. *J. Am. Chem. Soc.* **1994**, *116*, 11931–11937.
(92) Mantz, Y. A.; Gerard, H.; Iftimie, R.; Martyna, G. J. *J. Am. Chem. Soc.* **2004**, *126*, 4080–4081.
(93) Tomasi, J.; Mennucci, B.; Cammi, R. *Chem. Rev.* **2005**, *105*, 2999–3094.
(94) Frisch, M. J.; Trucks, G. W.; Schlegel, H. B.; Scuseria, G. E.; Robb, M. A.; Cheeseman, J. R.; Scalmani, G.; Barone, V.; Mennucci, B.; Petersson, G. A.; et al. *Gaussian 09, Revision A.1*; Gaussian, Inc.: Wallingford, CT, 2009.
(95) Westhof, E.; Sundaralingam, M. *J. Am. Chem. Soc.* **1983**, *105*, 970–976.
(96) Owens, N. W.; Lee, A.; Marat, K.; Schweizer, F. *Chem.—Eur. J.* **2009**, *15*, 10649–10657.
(97) Quiocho, F. A. *Annu. Rev. Biochem.* **1986**, *55*, 287–315.
(98) Vyas, N. K.; Vyas, M. N.; Quiocho, F. A. *Science (Washington, D.C.)* **1988**, *242*, 1290–1295.
(99) Cerny, J.; Hobza, P. *Phys. Chem. Chem. Phys.* **2007**, *9*, 5291–5303.
(100) Richardson, J. S. The Anatomy and Taxonomy of Protein Structure. In *Advances in Protein Chemistry*; Anfinsen, C. B., Edsall, J. T., Richards, F. M., Eds. Academic Press: 1981; Vol. 34, pp 167−339.
(101) Wilmot, C. M.; Thornton, J. M. *J. Mol. Biol.* **1988**, *203*, 221–232.
(102) Rose, G. D.; Glerasch, L. M.; Smith, J. A. Turns in Peptides and Proteins. In *Advances in Protein Chemistry*; Anfinsen, C. B., Edsall, J. T., Richards, F. M., Eds.; Academic Press: New York, 1985; Vol. 37, pp 1−109.
(103) Owens, N. W.; Braun, C.; O'Neil, J. D.; Marat, K.; Schweizer, F. *J. Am. Chem. Soc.* **2007**, *129*, 11670–11671.
(104) Bartlett, G. J.; Choudhary, A.; Raines, R. T.; Woolfson, D. N. *Nat. Chem. Biol.* **2010**, *6*, 615–620.
(105) Jakobsche, C. E.; Choudhary, A.; Miller, S. J.; Raines, R. T. *J. Am. Chem. Soc.* **2010**, *132*, 6651–6653.